ACS APPLIED MATERIALS & INTERFACES

Research Article

Cite This: ACS Appl. Mater. Interfaces 2020, 12, 2293−2298

www.acsami.org

Variable-Energy Hard X-ray Photoemission Spectroscopy: A Nondestructive Tool to Analyze the Cathode−Solid-State Electrolyte Interface

Yulong Liu,[†,#] Qian Sun,[†,#] Jingru Liu,[‡] Mohammad Norouzi Banis,[†] Yang Zhao,[†] Biqiong Wang,[†] Keegan Adair,[†] Yongfeng Hu,[§] Qunfeng Xiao,[§] Cheng Zhang,[‡] Li Zhang,[∥] Shigang Lu,[∥] Huan Huang,[⊥] Xiping Song,[*,‡] and Xueliang Sun[*,†]

[†]Department of Mechanical and Materials Engineering, University of Western Ontario, London N6A 5B9, Ontario, Canada

[‡]State Key Laboratory for Advance Metal and Materials, University of Science and Technology Beijing, Beijing 100083, China

[§]Canadian Light Source, Saskatoon S7N 2V3, Canada

[∥]China Automotive Battery Research Institute Company, Ltd, Beijing 100088, China

[⊥]Glabat Solid-State Battery Inc., 700 Collip Circle, Suite 211, London N6G 4X8, Ontario, Canada

Supporting Information

ABSTRACT: All-solid-state batteries are expected to be promising next-generation energy storage systems with increased energy density compared to the state-of-the-art Li-ion batteries. Nonetheless, the electrochemical performances of the all-solid-state batteries are currently limited by the high interfacial resistance between active electrode materials and solid-state electrolytes. In particular, elemental interdiffusion and the formation of interlayers with low ionic conductivity are known to restrict the battery performance. Herein, we apply a nondestructive variable-energy hard X-ray photoemission spectroscopy to detect the elemental chemical states at the interface between the cathode and the solid-state electrolyte, in comparison to the widely used angle-resolved (variable-angle) X-ray photoemission spectroscopy/X-ray absorption spectroscopy methods. The accuracy of variable-energy hard X-ray photoemission spectroscopy is also verified with a focused ion beam and high-resolution transmission electron microscopy. We also show the significant suppression of interdiffusion by building an artificial layer via atomic layer deposition at this interface.

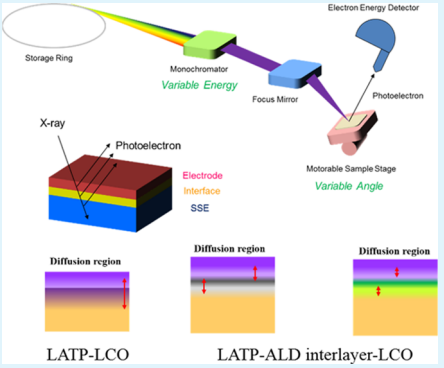

KEYWORDS: *solid-state battery, interface, ALD, X-ray photoemission spectroscopy, HRTEM*

INTRODUCTION

Lithium-ion batteries (LIBs) have been widely used in portable electronics and electric vehicles because of their high energy density and long durability. However, the conventional batteries contain flammable liquid electrolytes, leading to safety problems.[1,2] In addition, it is anticipated that the energy density of LIBs using liquid electrolytes will reach a limit in the near future based on the intercalation chemistry. Therefore, seeking new alternative energy storage systems is urgently required. Solid-state Li (-ion) batteries (SSLBs) have received great interest in recent years because of their intrinsic safety and higher energy density.[3,4] The use of a solid-state electrolyte (SSE), which is nonflammable, can be tolerant to extreme conditions. Additionally, Li metal is expected to be directly used as the anode in SSLBs to further increase their energy density.

Currently, the development and implementation of SSLBs are mostly hindered by the formation of resistive interfacial phenomena,[5] which can be typically summarized as physical mismatch, interfacial reactions, and space charge effects.[6−8] Among these interfacial phenomena, chemical/electrochemical reactions as well as elemental diffusions between the oxide electrode and oxide SSE at the interface are one of the most concerning problems that need to be overcome in SSLBs. In order to achieve a conjoined interface between these two oxide species that can facilitate facile ionic transportation, heat treatment (cosintering) is generally considered as an efficient approach.[9] However, the elemental interdiffusion between the cathode and oxide electrolyte during this high-temperature processing also has a negative effect on the performance of solid-state batteries.[9−11] Therefore, detecting the degree of elemental interdiffusion at the cathode−SE interface as well as developing an interlayer to suppress such diffusion is critical for the development of oxide SSLBs. Until now, the most widely used methods to probe these interfaces, for example, secondary ion mass spectrometry,[12] focused ion beam (FIB)

Received: September 10, 2019
Accepted: December 20, 2019
Published: December 20, 2019

DOI: 10.1021/acsami.9b16343
ACS Appl. Mater. Interfaces 2020, 12, 2293−2298

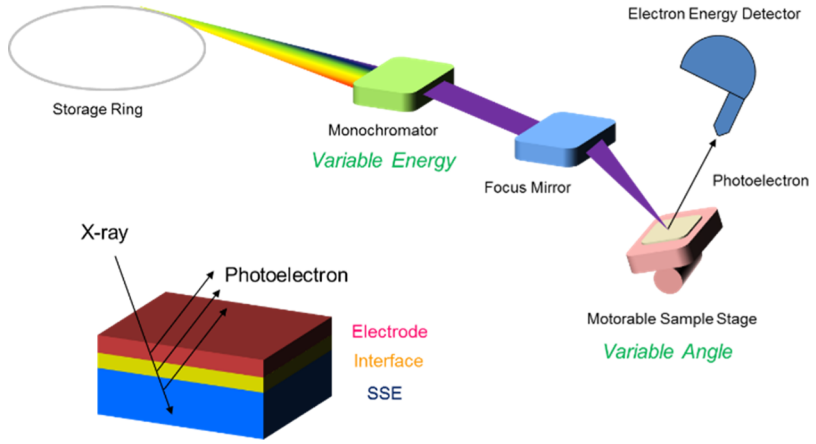

Figure 1. Schematic of synchrotron radiation-based VE-HAXPS.

combined with scanning electron microscopy/high-resolution transmission electron microscopy (HRTEM),[13] X-ray photoelectron spectroscopy (XPS) depth profiling via ion etching, are destructive to the samples. Therefore, it is of great research interest to develop a nondestructive (and in situ) detection tool for studying the interfaces in SSLBs. Okumura et al. applied depth-resolved X-ray absorption spectroscopy (XAS) with an angle-resolved two-dimensional pixel array fluorescence detector to reveal the formation of Co−Ti diffusion layer at the interface between $LiCoO_2$ (LCO) and $(Li_{1.3}Al_{0.3}Ti_{1.7}(PO_4)_3)$ (LATP) SSE,[14] whereas they also reported that NbO_2 layer was most effective among different oxide interlayers in restricting the side reactions because of the formation of the Li−Nb−O layer at the interface. Compared to XAS, XPS is surface-sensitive and suitable for the examination of interfaces. Janek and co-workers reported the use of in situ XPS to detect the side reactions between the lithium metal and SEs.[15−17] Moreover, in contrast to ion sputtering,[18] nondestructive XPS depth profiling can be realized by using variable energy and/or variable angle.[19,20]

In this paper, we will demonstrate the capability of nondestructive variable-energy hard X-ray photoemission spectroscopy (VE-HAXPS) to unveil the elemental interdiffusion at the interface between the directly deposited LCO thin-film cathode and the LATP SSE substrate with and without the introduction of an atomic layer deposition (ALD) interlayer between them. Afterward, we will also report the investigation of this interface using HRTEM coupled with an energy-dispersive system (EDS) to verify the accuracy of the results from VE-HAXPS.

RESULTS AND DISCUSSION

VE-HAXPS is an advanced XPS technology based on synchrotron radiation with tunable energy (Figure 1), which is able to provide high-energy monochromatic X-rays up to 10−15 keV comparing to the X-ray source for conventional lab XPS using Mg Kα (1253.6 eV) and Al Kα (1486.7 eV).[21] Accordingly, the excited photoelectrons have vastly increased the kinetic energy [kinetic energy (K.E.) = photon energy $h\nu$ − binding energy (B.E.) − work function (W.F.)] and thus significantly prolonged the escape depth. As a result, the detection depth of VE-HAXPS can transcend the limitation of conventional XPS and be able to reach several tens of nanometers depending on the photon energy and the element investigated.[22,23] The photoelectron escape depth is associated with the effective attenuation length/inelastic mean free path,[24] which can be simulated or experimentally measured to estimate the film thickness and composition evolution. Therefore, the depth-resolved chemical state/elemental composition distribution can be achieved using VE-HAXPS with tunable photon energies. The chemical information is collected along the surface to the buried interface and to bulk transition in a nondestructive way. These properties can be highly preferred for the studies on SSLBs.[14]

To demonstrate the capability of VE-HAXPS in SSLBs, we adopted an LATP SE and an LCO electrode layer as the model materials because of their research popularity in SSLBs and LIBs. It has been widely reported that the stability of the interface between the electrode/solid electrolytes has profound influence on the performance of the solid-state batteries.[9] Elemental cross-diffusion layers (interphase) have been observed at the interface of the solid electrolyte/electrode in solid-state batteries during the preparation process.[18,25,26] Usually, the formed interphase is a low ionic conductivity phase, which leads to capacity degradation. Therefore, we also seek to use a buffer layer at the interface between the solid electrolyte and the electrode fabricated by ALD in order to reduce the elemental interdiffusion at the interface region. Herein, Al_2O_3 and Li_3PO_4 were coated on the LATP solid electrolyte by ALD before the growth of LCO via sputtering and postannealing, respectively (Figures S1−S3).

The photon energies for VE-HAXPS have been selected as 3000, 4500, 6000, and 8000 eV to detect LATP, commercial LCO materials, LATP−LCO, LATP−Al_2O_3−LCO, and LATP−Li_3PO_4−LCO at different probing depths (Figure 2). O 1s spectra were chosen to analyze the composition distribution and degree of elemental diffusion because all the components (LCO, LATP, Al_2O_3, and Li_3PO_4) contain oxygen species, and each component can be differentiated from their O 1s XPS spectra. It can be observed that the main peaks of O 1s of LATP and LCO are located at 530.8 and 529.6 eV, respectively, which are in good agreement with the O 1s XPS of phosphate and lattice oxygen of LCO in the literature.[27,28] The 1.2 eV energy discrepancy between the O 1s XPS peaks facilitates the distinction of the LATP and LCO species from the spectra. From the O 1s spectra of the LATP−LCO sample collected at the photon energy of 3 keV, it can be clearly seen that two distinct peaks at 530.8 eV (from LATP) and 529.6 eV (from LCO) are present, indicating a strong diffusion of LATP into the LCO layer at a high temperature (as shown in Figure

DOI: 10.1021/acsami.9b16343
ACS Appl. Mater. Interfaces 2020, 12, 2293−2298

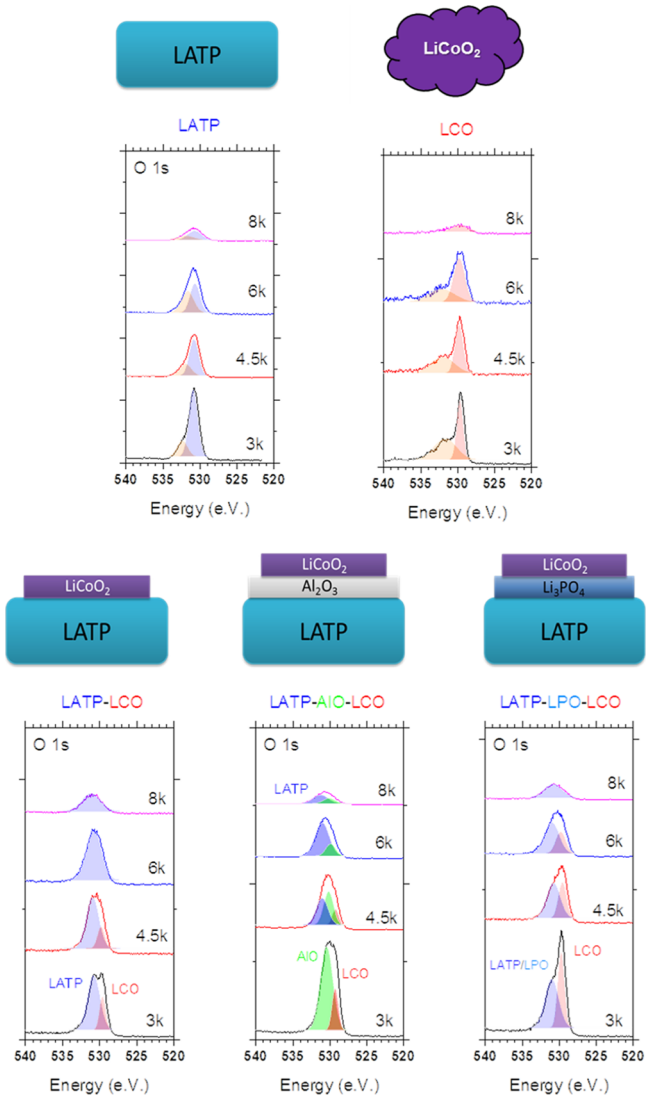

Figure 2. VE-HAXPS spectra of LATP, commercial LCO materials, LATP–LCO, LATP–Al_2O_3–LCO, and LATP–Li_3PO_4–LCO, using the photon energies of 3000 (3k), 4500 (4.5k), 6000 (6k), and 8000 (8k) eV, respectively.

S4). When the photon energy increased to 4.5k, 6k, and 8 keV, the intensity of the O 1s peak corresponding to the LCO lattice oxygen is significantly reduced, which corresponds to the deeper probing depth toward the bulk LATP buried under the LCO layer. In contrast, no obvious change can be found in the O 1s spectra of pure LATP and LCO, implying a consistent distribution of the surface and bulk composition/chemical states of these pristine materials.

To understand the effect of Al_2O_3 and Li_3PO_4 interlayers at the solid–solid interface, the chemical information of LATP–Al_2O_3–LCO and LATP–Li_3PO_4–LCO is investigated via VE-HAXPS. In the LATP–Al_2O_3–LCO sample (as shown in Figure 2), another O 1s peak appears at 530.20 eV. This energy value is in good agreement with the Al–O bond in Al_2O_3.[29] The O 1s peak intensity at 530.80 eV (O of LATP) is increased when the incident energy increases to 6k and 8k eV, implying the detection of the LATP signal underneath the surface LCO and Al_2O_3 layers. Nonetheless, the high intensity of the Al_2O_3 peak at the VE-HAXPS spectra at the surface (3k and 4.5k eV) indicates that the Al_2O_3 layer, instead of LATP, had intensively interdiffused into the LCO layer under a high-temperature treatment. In contrast, the O 1s VE-HAXPS spectra of LATP–Li_3PO_4–LCO at 3 keV shows very sharp features from the LCO lattice oxygen with a minor contribution from the oxygen in phosphate (LATP and/or Li_3PO_4, which cannot be distinguished herein). With the increasing detecting depth, the change from the LCO lattice oxygen peak to oxygen in the phosphate peak can be found in the VE-HAXPS spectra. These results doubtlessly suggest that ALD Li_3PO_4 can efficiently prevent the elemental interdiffusion between the LATP SSE and the LCO electrode layer, which may be anticipated to be a preferred interlayer for the SSLB assembly.

In order to verify the accuracy of VE-HAXPS results and obtain more physical–chemical information on the elemental interdiffusion, the LATP–LCO, LATP–Al_2O_3–LCO, and LATP–Li_3PO_4–LCO samples are sliced by FIB and their cross-sectional images are collected by HRTEM. The cross-sectional TEM images and the chemical information of the interfaces are shown in Figure 3. From the TEM cross-sectional images in Figure 3a, an anomalous contrast layer is presented at the pristine LATP–LCO interface. The details of these interfaces were evaluated by EDS mapping and line-scans. From the EDS mapping, Co and Ti elements account for the regions of the LCO electrode and the LATP electrolyte, respectively. In the line profile, it is revealed that the thickness of the LCO thin film (estimated based on the Co element) is 80 nm in total. In the vicinity of the LCO thin film and LATP bulk electrolyte, there is a region of intermediate layer consisting of both Co and Ti elements. The intermediate layer thickness is 60 nm, originating from the mutual diffusion between LATP and LCO at a high temperature. When an interlayer of Al_2O_3 is inserted at the LATP–LCO interface, as shown in Figure 3b, an obvious Al element mapping is observed in EDS mapping. More importantly, the thickness of LCO is reduced to 50 nm, as calculated from the EDS line profile. In addition, the EDS line profile shows some changes across the modified interfacial region. Instead of a Co–Ti diffusion region, there are two interdiffused regions which are formed at the LATP–Al_2O_3–LCO interface. The first region is the Co–Al region where the intensity of Co decreases with distance, whereas the intensity of Al increases, with a thickness of 20 nm. On the surface of the Al_2O_3-coated LATP electrolyte, Ti is diffused into the Al_2O_3 layer at a high temperature, forming a layer with a thickness of about 12 nm. To confirm the accuracy of the diffusion zone, an electron energy loss spectroscopy (EELS) line scan at the LATP–Al_2O_3–LCO interface is performed, and the result is presented in Figure S5. Consistent with the EDX result, the EELS line scan also shows two cross-diffusion zones, with thicknesses of 15 and 12 nm, respectively. In the case of LATP–Li_3PO_4–LCO, no Li_3PO_4 layer is observed at the interface from the EDS mapping in Figure 3c. This can be partially attributed to the similar chemical composition of LATP and Li_3PO_4 coatings. Compared with the LATP–Al_2O_3–LCO interface, the thickness of LCO is further reduced to only 35 nm, which is almost half of the pristine LATP–LCO. Additionally, the diffused region is reduced to only 10 nm, where Ti, Co, and P coexisted. Ti is diffused into the Li_3PO_4 layer as well, as seen on the surface of LATP–Li_3PO_4 (as marked by a gray rectangle), with a layer thickness of 20 nm. From both VE-HAXPS and FIB-HRTEM/EDS results, it can be concluded that the ALD layer is able to control the elemental diffusion

DOI: 10.1021/acsami.9b16343
ACS Appl. Mater. Interfaces 2020, 12, 2293–2298

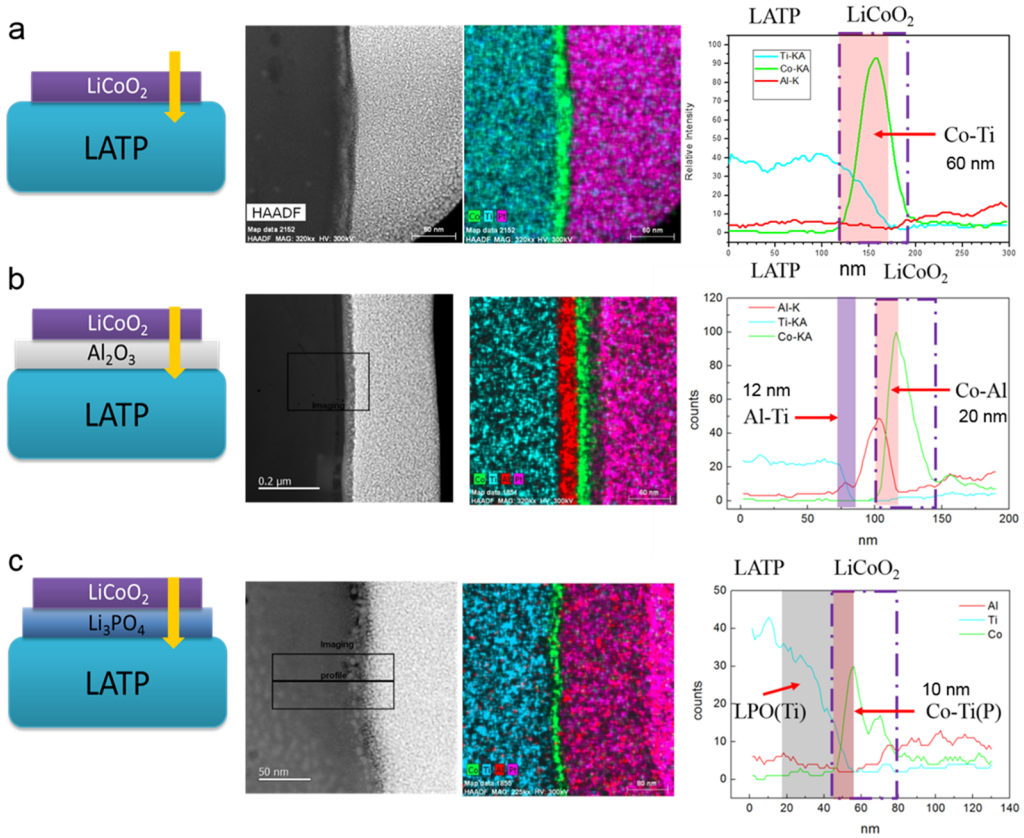

Figure 3. Cross-sectional image of the interface of (a) LATPLCO, (b) LATP−Al_2O_3−LCO, and (c) LATP−Li_3PO_4−LCO by FIB-HRTEM/EDX.

phenomenon at the cathode/electrolyte interface, and the ALD Li_3PO_4 layer is more effective in preventing Co diffusion into the electrolyte (as shown in Figure 4).

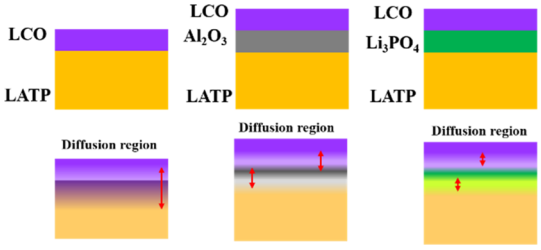

Figure 4. Overall schematic of the elemental diffusion between LCO and LATP.

The LiPON−LCO interface was thought to be very stable, and no side reaction happened at the interface. However, Meng's group obtained the evidence of Li accumulation at the interface by the combination of STEM/EELS information, which accounted for the irreversible capacity losses in long cycles.[30] They detected an intermediate layer at the LiPON−LCO interface by combing a sputtering machine with the in situ XPS analysis system in one vacuum chamber, and some new species were detected and changed with the growing layer thickness of LiPON.[31] If HE-HAXPS is applied at the LiPON−LCO interface, there is a possibility to detect such chemical information without complex in situ instruments. A mutual diffusion phenomenon is more obvious in the sulfide solid electrolyte/oxide electrode interface because of its low stability against a high-voltage cathode. Sakuda and co-workers observed a mutual diffusion layer formed at the interface of Li_2S−P_2S_5−LCO using high-angle annular dark field microscopy/EELS, and the layer consisted of Co, P, and S.[32] The diffusion phenomenon is accelerated at a higher temperature; an interface layer of 300 nm is formed after pressing LCO with Li_2S−P_2S_5 at 210 °C, whereas no interface overserved at room temperature.[33] From theoretical calculations, it is observed that a CoS_2-rich interphase was plausible at the Li_3PS_4−LCO interface.[34] Although the intermediate compounds are predicted from the chemical potential diagrams, the detailed chemical information of interphases at the interfaces of sulfide/electrode is hard to be detected by experiment except the STEM/EELS technique. With the help of HE-HAXPS, the interdiffusion phenomenon across the interface can be further investigated without destroying the nature of interface by the electron beam.

CONCLUSIONS

Overall, we demonstrate the applicability and potential of VE-HAXPS as a powerful nondestructive tool to probe the elemental diffusion at the interfaces in SSLB, which reveals the interface results consistent with the observation with the destructive FIB-HRTEM/EDS method. Furthermore, we demonstrate the effectiveness of different ALD interlayer modifications on suppressing the elemental diffusion. Li_3PO_4 is found to have a positive effect on stabilizing the LATP−LCO interface.

ASSOCIATED CONTENT

Supporting Information

The Supporting Information is available free of charge at https://pubs.acs.org/doi/10.1021/acsami.9b16343.

DOI: 10.1021/acsami.9b16343
ACS Appl. Mater. Interfaces 2020, 12, 2293−2298

Experimental details and additional physical and electrochemical characterizations (PDF)

AUTHOR INFORMATION

Corresponding Authors

*E-mail: xpsong@skl.ustb.edu.cn (X.S.).
*E-mail: xsun9@uwo.ca (X.S.).

ORCID

Mohammad Norouzi Banis: 0000-0002-6144-6837
Biqiong Wang: 0000-0002-3903-8634
Xueliang Sun: 0000-0003-0374-1245

Author Contributions

#Y.L. and Q.S. contributed equally to this manuscript.

Notes

The authors declare no competing financial interest.

ACKNOWLEDGMENTS

This research was supported by the China Automotive Battery Research Institute, Beijing, Nature Science and Engineering Research Council of Canada (NSERC), the Canada Research Chair Program (CRC), Canada Foundation for Innovation (CFI), the Canadian Light Sources (CLS), and the University of Western Ontario. Q.S. and B.W. acknowledge the receipt of the CLS Postdoctoral Student Travel Support Program. Q.S. appreciates the support of the MITACS Elevate postdoctoral program. J.L., C.Z., and X.S. acknowledge the support of State Key Lab of Advanced Metals and Materials, University of Science and Technology Beijing, Beijing, China.

REFERENCES

(1) Takada, K. Progress and Prospective of Solid-State Lithium Batteries. *Acta Mater.* **2013**, *61*, 759−770.
(2) Sun, C.; Liu, J.; Gong, Y.; Wilkinson, D. P.; Zhang, J. Recent Advances in All-Solid-State Rechargeable Lithium Batteries. *Nano Energy* **2017**, *33*, 363−386.
(3) Xu, K. Electrolytes and Interphases in Li-Ion Batteries and Beyond. *Chem. Rev.* **2014**, *114*, 11503−11618.
(4) Chen, R.; Qu, W.; Guo, X.; Li, L.; Wu, F. The Pursuit of Solid-State Electrolytes for Lithium Batteries: From Comprehensive Insight to Emerging Horizons. *Mater. Horiz.* **2016**, *3*, 487−516.
(5) Richards, W. D.; Miara, L. J.; Wang, Y.; Kim, J. C.; Ceder, G. Interface Stability in Solid-State Batteries. *Chem. Mater.* **2016**, *28*, 266−273.
(6) Sakuma, M.; Suzuki, K.; Hirayama, M.; Kanno, R. Reactions at the Electrode/Electrolyte Interface of All-Solid-State Lithium Batteries Incorporating Li−M (M=Sn, Si) Alloy Electrodes and Sulfide-Based Solid Electrolytes. *Solid State Ionics* **2016**, *285*, 101−105.
(7) Tsai, C.-L.; Roddatis, V.; Chandran, C. V.; Ma, Q.; Uhlenbruck, S.; Bram, M.; Heitjans, P.; Guillon, O. $Li_7La_3Zr_2O_{12}$ Interface Modification for Li Dendrite Prevention. *ACS Appl. Mater. Interfaces* **2016**, *8*, 10617−10626.
(8) Haruyama, J.; Sodeyama, K.; Han, L.; Takada, K.; Tateyama, Y. Space−Charge Layer Effect at Interface between Oxide Cathode and Sulfide Electrolyte in All-Solid-State Lithium-Ion Battery. *Chem. Mater.* **2014**, *26*, 4248−4255.
(9) Park, K.; Yu, B.-C.; Jung, J.-W.; Li, Y.; Zhou, W.; Gao, H.; Son, S.; Goodenough, J. B. Electrochemical Nature of the Cathode Interface for a Solid-State Lithium-Ion Battery: Interface between $LiCoO_2$ and Garnet-$Li_7La_3Zr_2O_{12}$. *Chem. Mater.* **2016**, *28*, 8051−8059.
(10) Kim, K. H.; Iriyama, Y.; Yamamoto, K.; Kumazaki, S.; Asaka, T.; Tanabe, K.; Fisher, C. A. J.; Hirayama, T.; Murugan, R.; Ogumi, Z. Characterization of the Interface between $LiCoO_2$ and $Li_7La_3Zr_2O_{12}$ in an All-Solid-State Rechargeable Lithium Battery. *J. Power Sources* **2011**, *196*, 764−767.
(11) Kato, T.; Hamanaka, T.; Yamamoto, K.; Hirayama, T.; Sagane, F.; Motoyama, M.; Iriyama, Y. In-Situ $Li_7La_3Zr_2O_{12}/LiCoO_2$ Interface Modification for Advanced All-Solid-State Battery. *J. Power Sources* **2014**, *260*, 292−298.
(12) Li, Y.; Chen, X.; Dolocan, A.; Cui, Z.; Xin, S.; Xue, L.; Xu, H.; Park, K.; Goodenough, J. B. Garnet Electrolyte with an Ultralow Interfacial Resistance for Li-Metal Batteries. *J. Appl. Chem. Sci.* **2018**, *140*, 6448−6455.
(13) Choi, S.; Jeon, M.; Ahn, J.; Jung, W. D.; Choi, S. M.; Kim, J.-S.; Lim, J.; Jang, Y.-J.; Jung, H.-G.; Lee, J.-H.; Sang, B.-I.; Kim, H. Quantitative Analysis of Microstructures and Reaction Interfaces on Composite Cathodes in All-Solid-State Batteries Using a Three-Dimensional Reconstruction Technique. *ACS Appl. Mater. Interfaces* **2018**, *10*, 23740−23747.
(14) Okumura, T.; Nakatsutsumi, T.; Ina, T.; Orikasa, Y.; Arai, H.; Fukutsuka, T.; Iriyama, Y.; Uruga, T.; Tanida, H.; Uchimoto, Y.; Ogumi, Z. Depth-Resolved X-Ray Absorption Spectroscopic Study on Nanoscale Observation of the Electrode−Solid Electrolyte Interface for All Solid State Lithium Ion Batteries. *J. Mater. Chem.* **2011**, *21*, 10051.
(15) Wenzel, S.; Leichtweiss, T.; Krüger, D.; Sann, J.; Janek, J. Interphase Formation on Lithium Solid Electrolytes-an in Situ Approach to Study Interfacial Reactions by Photoelectron Spectroscopy. *Solid State Ionics* **2015**, *278*, 98−105.
(16) Wenzel, S.; Randau, S.; Leichtweiß, T.; Weber, D. A.; Sann, J.; Zeier, W. G.; Janek, J. Direct Observation of the Interfacial Instability of the Fast Ionic Conductor $Li_{10}GeP_2S_{12}$ at the Lithium Metal Anode. *Chem. Mater.* **2016**, *28*, 2400−2407.
(17) Wenzel, S.; Weber, D. A.; Leichtweiss, T.; Busche, M. R.; Sann, J.; Janek, J. Interphase Formation and Degradation of Charge Transfer Kinetics between a Lithium Metal Anode and Highly Crystalline $Li_7P_3S_{11}$ Solid Electrolyte. *Solid State Ionics* **2016**, *286*, 24−33.
(18) Zarabian, M.; Bartolini, M.; Pereira-Almao, P.; Thangadurai, V. X-Ray Photoelectron Spectroscopy and Ac Impedance Spectroscopy Studies of Li-La-Zr-O Solid Electrolyte Thin Film/$LiCoO_2$ Cathode Interface for All-Solid-State Li Batteries. *J. Electrochem. Soc.* **2017**, *164*, A1133−A1139.
(19) Sachs, M.; Gellert, M.; Chen, M.; Drescher, H.-J.; Kachel, S. R.; Zhou, H.; Zugermeier, M.; Gorgoi, M.; Roling, B.; Gottfried, J. M. $LiNi_{0.5}Mn_{1.5}O_4$ High-Voltage Cathode Coated with $Li_4Ti_5O_{12}$: A Hard X-Ray Photoelectron Spectroscopy (Haxpes) Study. *Phys. Chem. Chem. Phys.* **2015**, *17*, 31790−31800.
(20) Vardar, G.; Bowman, W. J.; Lu, Q.; Wang, J.; Chater, R. J.; Aguadero, A.; Seibert, R.; Terry, J.; Hunt, A.; Waluyo, I. Structure, Chemistry, and Charge Transfer Resistance of the Interface between $Li_7La_3Zr_2O_{12}$ Electrolyte and $LiCoO_2$ Cathode. *Chem. Mater.* **2018**, *30*, 6259−6276.
(21) Fadley, C. S. X-Ray Photoelectron Spectroscopy and Diffraction in the Hard X-Ray Regime: Fundamental Considerations and Future Possibilities. *Nucl. Instrum. Methods Phys. Res., Sect. A* **2005**, *547*, 24−41.
(22) Rubio-Zuazo, J.; Castro, G. R. Information Depth Determination for Hard X-Ray Photoelectron Spectroscopy up to 15 Kev Photoelectron Kinetic Energy. *Surf. Interface Anal.* **2008**, *40*, 1438−1443.
(23) Risterucci, P.; Renault, O.; Martinez, E.; Detlefs, B.; Delaye, V.; Zegenhagen, J.; Gaumer, C.; Grenet, G.; Tougaard, S. Probing Deeper by Hard X-Ray Photoelectron Spectroscopy. *Appl. Phys. Lett.* **2014**, *104*, 051608.
(24) Jablonski, A.; Powell, C. J. Relationships between Electron Inelastic Mean Free Paths, Effective Attenuation Lengths, and Mean Escape Depths. *J. Electron Spectrosc. Relat. Phenom.* **1999**, *100*, 137−160.
(25) Ohta, S.; Seki, J.; Yagi, Y.; Kihira, Y.; Tani, T.; Asaoka, T. Co-Sinterable Lithium Garnet-Type Oxide Electrolyte with Cathode for All-Solid-State Lithium Ion Battery. *J. Power Sources* **2014**, *265*, 40−44.

DOI: 10.1021/acsami.9b16343
ACS Appl. Mater. Interfaces 2020, 12, 2293−2298

(26) Van den Broek, J.; Afyon, S.; Rupp, J. L. M. Interface-Engineered All-Solid-State Li-Ion Batteries Based on Garnet Type Fast Li^+ Conductors. *Adv. Energy Mater.* **2016**, *6*, 1600736−1600747.
(27) Dobbelaere, T.; Mattelaer, F.; Dendooven, J.; Vereecken, P.; Detavernier, C. Plasma-Enhanced Atomic Layer Deposition of Iron Phosphate as a Positive Electrode for 3d Lithium-Ion Microbatteries. *Chem. Mater.* **2016**, *28*, 3435−3445.
(28) Verdier, S.; El Ouatani, L.; Dedryvère, R.; Bonhomme, F.; Biensan, P.; Gonbeau, D. XPS Study on Al_2O_3-and $AlPO_4$-Coated $LiCoO_2$ Cathode Material for High-Capacity Li Ion Batteries. *J. Electrochem. Soc.* **2007**, *154*, A1088−A1099.
(29) Iatsunskyi, I.; Kempiński, M.; Jancelewicz, M.; Załęski, K.; Jurga, S.; Smyntyna, V. Structural and XPS Characterization of ALD Al_2O_3 Coated Porous Silicon. *Vacuum* **2015**, *113*, 52−58.
(30) Santhanagopalan, D.; Qian, D.; McGilvray, T.; Wang, Z.; Wang, F.; Camino, F.; Graetz, J.; Dudney, N.; Meng, Y. S. Interface Limited Lithium Transport in Solid-State Batteries. *J. Phys. Chem. Lett.* **2014**, *5*, 298−303.
(31) Jacke, S.; Song, J.; Cherkashinin, G.; Dimesso, L.; Jaegermann, W. Investigation of the Solid-State Electrolyte/Cathode Lipon/Licoo2 Interface by Photoelectron Spectroscopy. *Ionics* **2010**, *16*, 769−775.
(32) Sakuda, A.; Hayashi, A.; Tatsumisago, M. Interfacial Observation between $LiCoO_2$electrode and Li_2S−P_2S_5solid Electrolytes of All-Solid-State Lithium Secondary Batteries Using Transmission Electron Microscopy. *Chem. Mater.* **2010**, *22*, 949−956.
(33) Kitaura, H.; Hayashi, A.; Ohtomo, T.; Hama, S.; Tatsumisago, M. Fabrication of Electrode Electrolyte Interfaces in All-Solid-State Rechargeable Lithium Batteries by Using a Supercooled Liquid State of the Glassy Electrolytes. *J. Mater. Chem.* **2011**, *21*, 118−124.
(34) Yokokawa, H. Thermodynamic Stability of Sulfide Electrolyte/Oxide Electrode Interface in Solid-State Lithium Batteries. *Solid State Ionics* **2016**, *285*, 126−135.

DOI: 10.1021/acsami.9b16343
ACS Appl. Mater. Interfaces 2020, 12, 2293−2298